Temporal evolution of sediment supply in Lago Puyehue (Southern Chile) during the last 600 yr and its climatic significance

Sébastien Bertrand[a], Xavier Boës[a], Julie Castiaux[a], François Charlet[b], Roberto Urrutia[c], Cristian Espinoza[c], Gilles Lepoint[d], Bernard Charlier[e], Nathalie Fagel[a]

[a]*Clays and Paleoclimate Research Unit, Department of Geology, University of Liège, Allée du 6 août, B18, 4000 Liège, Belgium*
[b]*Renard Centre of Marine Geology (RCMG), University of Ghent, 9000 Ghent, Belgium*
[c]*Centro EULA, University of Concepción, Concepción, Chile*
[d]*Marine Research Centre (MARE), Laboratory of Oceanology, University of Liège, 4000 Liège, Belgium*
[e]*Endogenous Petrology and Geochemistry Research Unit, University of Liège, 4000 Liège, Belgium*

Abstract

Short-term climate changes in Southern Chile are investigated by a multi-proxy analysis of a 53-cm-long sedimentary sequence selected among eight short cores retrieved in Lago Puyehue (Chile, 40°S). This core contains a 600-yr-long undisturbed record of paleo-precipitation changes. Two measurement methods for sediment density, organic matter and biogenic silica contents are compared and the most appropriate techniques are selected. Together with aluminium and titanium concentrations, grain size and geochemical properties of the organic matter, these proxies are used to demonstrate paleo-precipitation changes around 40°S. Increase of terrigenous particle supply between A.D. 1490 and A.D. 1700 suggests a humid period. Contemporaneously, $\delta^{13}C$ data show increasing lake productivity, in response to the high nutrient supply. The A.D. 1700-1900 interval is characterized by a decreasing terrigenous supply and increasing $\delta^{13}C$ values, interpreted as a drying period. The magnetic susceptibility signal, reflecting the terrigenous/biogenic ratio, demonstrates that similar variations occur in all the undisturbed sedimentary environments of Lago Puyehue. The A.D. 1490-1700 wet period is associated with the onset of the European Little Ice Age (LIA) and interpreted as its local signature. This work supports the fact that the LIA was a global event, not only restricted to the Northern Hemisphere.

Keywords: Southern Chile ; last millennium ; paleolimnology ; Little Ice Age ; sediments

Introduction

Paleoclimate data from the Southern Hemisphere are still insufficient to allow a detailed reconstruction of the last millennium (e.g., Markgraf, 2001; Committee on Abrupt Climate Change, 2002). However, Southern Hemisphere climate records could provide relevant clues to the mechanisms that underlie interhemispheric teleconnections and global climatic changes (Lara and Villalba, 1993). Southern Chile is a key site to understand past climatic variations since it is located at the windward side of the Andes and at the northern limit of the Southern Westerlies influence, making the area very sensitive to variations of these humidity-bearing winds. Moreover, it is far removed from the direct influence of Northern Hemisphere ice sheets and North Atlantic thermohaline circulation. Until now, most of the evidence for climate variability in the Southern Hemisphere over the last millennium comes from tree rings, supplemented by a few ice cores and speleothems, as well as corals records (for a review, see Bradley et al., 2003). For the Chilean Lake District, lake sediments represent an excellent archive of environmental and climate variability. Because of high sedimentation rates (~1 mm/yr), lake deposits can be studied with a decadal resolution.

In Northern Patagonia, two periods of glacial advances, probably linked to a cold climate, were recognized at A.D. 1270-1380 and A.D. 1520-1670 (Villalba, 1990, 1994; Lara and Villalba, 1993; Luckman and Villalba, 2001). In Peru, Thompson et al. (1986) described a cold period (i.e., the Little Ice Age) between A.D. 1530 and A.D. 1900 from the oxygen isotopes study of the Quelccaya ice core. However, they demonstrated that this interval is characterized by humidity changes: wet from A.D. 1520 to A.D. 1720 and dry from A.D. 1720 to A.D. 1860 (Thompson et al., 1985).

The aims of this paper are as follows: (1) to compare different methods for the measurement of density, organic matter and biogenic silica contents of the sediment and select the most appropriate techniques for analyzing sediment from Lago Puyehue; and (2) to apply the selected methods together with other proxies on short cores to
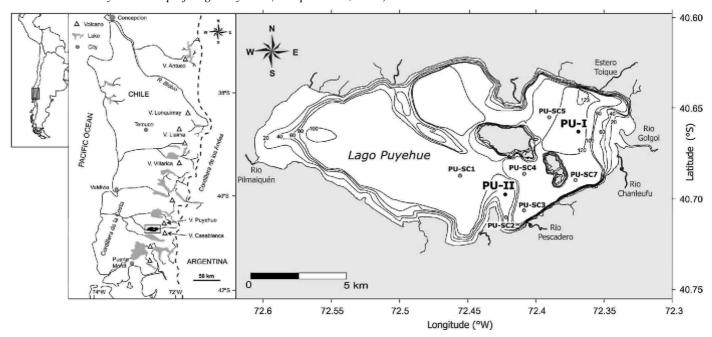
infer climate variability for the last 600 yr in the Southern Hemisphere.

Location and setting

Lago Puyehue (40.70°S, 72.45°W) is located in the foothills of the Cordillera de Los Andes at an elevation of 185 m.a.s.l. (Fig. 1). With a surface of 164 km^2 and a maximum depth of 123 m, it constitutes a typical oligotrophic moraine-dammed lake in the Chilean Lake District (38-43°S; Campos et al., 1989). This lake lies in an overdeepened glacial valley shaped during Quaternary glacial advances (Laugenie, 1982). Its watershed covers 1267 km^2 and mainly consists of Quaternary volcanic rocks covered by plurimetric post-glacial andosoils (i.e., the Trumaos) (Laugenie, 1982). It is surrounded by several active volcanoes: Puyehue-Cordon de Caulle and Casablanca volcanic complexes, peaking at 2240 and 1990 m.a.s.l., respectively. The last eruption of Puyehue-Cordon de Caulle volcanic complex is linked to the 1960 Valdivia earthquake. Lago Puyehue is fed by Rio Golgol from the East, forming the main delta of the lake, and by several smaller rivers (Fig. 1). The outlet of Lago Puyehue (Rio Pilmaiquen), which cross-cuts several moraine ridges (Laugenie, 1982; Bentley, 1997), merges with Rio Bueno and flows westward into the Pacific. At 6 km downstream from Lago Puyehue, Rio Pilmaiquen has been dammed by a hydroelectric plant since 1944.

Present-day local climate is characterized by humid temperate conditions with year round precipitations peaking in the austral winter (Miller, 1976; Heusser, 2003). Precipitations are driven by the Southern Westerlies and their seasonal shifts. The rough topography of the Cordillera de Los Andes forms an effective barrier to the Westerlies and receives most of the precipitations. Annual precipitation increases with elevation and varies from 2000 mm/yr around the lake to 5000 mm/yr on the top of regional volcanoes (Parada, 1973). Mean annual temperature is 6° to 9°C, with a maximum of 20°C in January and a minimum of 2°C in July (Muñoz, 1980). The lake productivity is mainly phosphorous limited. Its high silica concentration (15 mg/l; Campos et al., 1989) is characteristic for lakes located in volcanic settings.

Figure 1: Location of Lago Puyehue among the Chilean Lake District. Short cores collection sites are indicated on the bathymetric map of Lago Puyehue (Campos et al., 1989). Isobath = 20 m.

Material

Coring and core processing

Two main coring sites were selected by a preliminary seismic investigation of the lake infilling. Site PU-I is located at 122.4 m depth and faces the Golgol delta, where sedimentary environments are under the influence of Golgol river underflows (Fig. 1). PU-II is situated on a subaquatic moraine ridge at 48.4 m depth, where sedimentation is dominated by interflow deposits. At each site, five short cores were taken using a Uwitec platform and a short gravity coring device. In addition, six secondary sites were selected for short gravity coring (PU-SC1 to PU-SC7; Fig. 1). After core opening and description, the working half of each core was subsampled by cutting 1-cm-thick slices. Core lengths vary between 16 and 88.5 cm (Table 1). Some compaction is observed between the five short cores of PU-I and PU-II coring sites (1-13%).

Lithology

Core lithology is characterized by homogeneous to finely laminated silt-sized sediment composed of terrigenous particles, diatoms and organic matter in variable proportions (Fig. 2). Microscopic study of smear slides reveals that diatoms occur throughout the cores. This characteristic is typical for lakes located in volcanic settings (e.g., Lago Grande di Monticchio; Robinson, 1994). The main diatom taxa are *Aulacoseira* and *Cyclotella.* We focused our work on PU-II site because it contains a continuous sedimentary record (Fig. 2). In addition, this site has been selected for long-core drilling and long-term climate reconstructions (Bertrand, 2005). The PU-II short core contains two fine green layers at 5-5.5 cm and 9-10 cm and two coarse sandy tephra layers at 13.5-13.8 cm and 43-43.5 cm depth (Fig. 3). These four particular layers, recognized in nearly all cores, are used as stratigraphic markers for core correlation (Fig. 2). These correlations are strengthened by magnetic susceptibility results and by mineralogical characteristics of tephra layers. According to thin sections, the sediments of PU-II short core are annually laminated throughout, except between 3.5 and 7 cm where an unstratified layer occurs. This remobilization layer occurs in all short cores but its signature depends on the dominant sedimentation pattern (i.e., turbidite deposit, destratified layer, etc.). We worked on two short cores collected 2 m distant from each other (PU-II-P1 and PU-II-P5). A mean relative compaction of 7.5% between both records has been deduced from correlations using the four previously described stratigraphic markers. The age-depth model realized on PU-II-P5 core is used as a chronologic reference and data obtained on PU-II-P1 core (grain size and point sensor magnetic susceptibility) have been depth adjusted. All other proxies were measured on PU-II-P5.

Table 1: *Location and characteristics of the eight coring sites in Lago Puyehue*

Site number	Latitude (°S)	Longitude (°W)	Depth (m)	Core length (cm)
PU-I	40°39.766'	72°22.155'	122.4	56-63
PU-II	40°41.843'	72°25.341'	48.4	47.5-52.5
PU-SC1	40°41.261'	72°27.337'	90	55.2
PU-SC2	40°42.645'	72°25.311'	53.6	67
PU-SC3	40°42.418'	72°24.527'	110.2	72.3
PU-SC4	40°41.194'	72°24.521'	108.8	88.5
PU-SC5	40°39.302'	72°23.447'	115	16
PU-SC7	40°41.407'	72°22.261'	113.5	80

Age-depth model

Age-depth model of PU-II short core was established by varve counting and further calibrated by ^{210}Pb and ^{137}Cs dating and recognition of historical events (F Arnaud and O. Magand, unpublished data). Sedimentation rates vary from 0.7 to 1.7 mm/yr (Fig. 3). One-centimeter-thick samples thus represent 6 to 14 yr. The two green layers in PU-II short core are dated at A.D. 1960 and A.D. 1944. The coarse tephra layers are related to the A.D. 1921-1922 eruption of Puyehue-Cordon de Caulle and the A.D. 1575 eruption of Osorno Volcano. The non-stratified sediment layer (3.5-7 cm) is an event deposit related to the 1960 Valdivia earthquake.

Figure 2: *Magnetic susceptibility results (10^{-6} S.I.) and correlations between the 8 short cores collected in Lago Puyehue. For coring location, see Figure 1. Reference layers are deduced from (1) macroscopic description, (2) mineralogy of tephra layers, (3) magnetic susceptibility peaks and (4) recognition of event deposits. The upper tephra (13.5 -13.8 cm in PU-II) is dominated by orthopyroxene while the lower tephra (43-43.5 cm in PU-II) is dominated by olivine and orthopyroxene. The 4 cores collected west of Fresia and Cuicui islands and represented on the left side of the figure contain an undisturbed sedimentary record. PU-SC3, PU-SC7 and PU-I P4 cores, collected on sedimentary environments influenced by Golgol or Pescadero river underflows, contain an unstratified layer related to the 1960 Valdivia earthquake. The contemporaneous eruption of Puyehue-Cordon de Caulle volcanic complex is responsible for the deposition of volcanic ash or pumices, actually weathered into a green clay layer.*
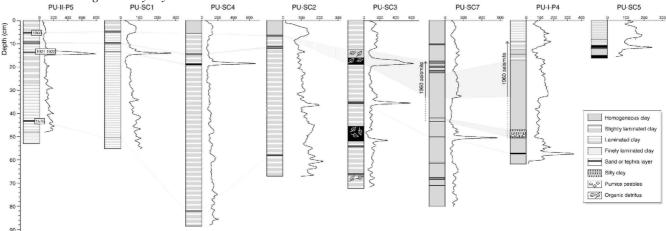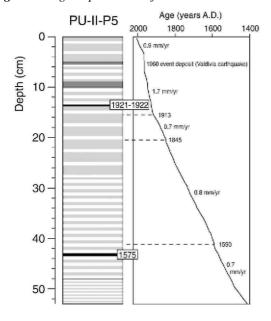

Figure 3: *Age-depth model of PU-II short core derived from varve counting.*

Methods

Physical parameters and loss on ignition

Before opening, all the cores were scanned for magnetic susceptibility and gamma-density with a Geotek multisensor track. Moreover, magnetic susceptibility was measured on opened cores with a Bartington MS2E point sensor every 5 mm.

Loss on ignition (LOI) was measured after 24 h at 105°C (water content, density), after 4 h at 550°C and after 2 h at 950°C following Herri et al. (2001). Replicates for LOI_{105} show very good results ($r^2 = 0.97$, $P < 0.0001$). Because LOI_{550} precision depends on the initial sample weight (Herri et al., 2001), analyses were systematically performed on 1 g of dry samples (0.98 ± 0.03 g).

Grain size

Grain size measurements were performed on bulk sediment using a laser diffraction particle analyzer Malvern Mastersizer 2000 detecting a 0.02- to 2000-µm size range. Samples were introduced into a 100-ml demonized water tank free of additive dispersant, split with a 2000-rpm stirrer and crumbled with ultrasonic waves. Sample quantity was adjusted in order to obtain a laser beam obscuration between 10% and 20%. Grain size parameters were averaged over 10,000 scans. Samples containing grains coarser than 420 µm were analyzed by a combination of laser diffraction and sieving methods. These samples were separated by wet sieving at 420 µm and freeze dried. The finest sediment was analyzed by laser diffraction and the coarsest by dry sieving. Both results were then joined after correction of their relative weight to form a continuous grain size distribution. Distribution parameters were calculated following Folk and Ward (1957).

Mineralogy

Bulk mineralogy was analyzed by X-ray diffraction (XRD) on a Bruker D8-Advance diffractometer with CuKα radiations. Bulk samples were powdered to 100 µm using an agate mortar. An aliquot was separated and mounted as unoriented powder by the backside method (Brindley and Brown, 1980). The powder was scanned by XRD between 2° and 45° 2θ. The data were analyzed in a semiquantitative way following Cook et al. (1975). The intensity of the principal peak of each mineral was measured and corrected by a multiplication factor. For amorphous material, a mean correction factor was obtained from diffraction results on mixtures of known quantities of amorphous material and quartz. We calculated a mean correction factor of 75, applied to the maximum of the broad diffraction band at 3.7 Å.

Geochemistry

Major elements of PU-II short core were analyzed at 1-cm resolution by X-ray fluorescence on Li-borate glass after loss on ignition at 950°C. Analyses were performed on an ARL 9400. The relative accuracy is 0.50%, 3.07% and 1.69% for SiO_2, TiO_2 and Al_2O_3, respectively (Bologne and Duchesne, 1991). Biogenic silica is determined by normative calculation (Leinen, 1977):

$$SiO_2\, bio(\%) = SiO_2\, tot(\%) - x \cdot Al_2O_3(\%)$$

where x is the SiO_2/Al_2O_3 ratio of terrigenous sediments. Soils and rocks in the lake catchment are expected to represent the main sources of lacustrine terrigenous particles. Their SiO_2/Al_2O_3 ratio was calculated by XRF.

Moreover, biogenic silica was extracted by Na_2CO_3 and quantified by blue spectrophotometry (Mortlock and Froelich, 1989). Results are given in weight percent of biogenic SiO_2. Precision ranges from $\pm 4\%$ to $\pm 8\%$, depending on the biogenic silica concentration (Mortlock and Froelich, 1989).

Total organic carbon (TOC) and total organic nitrogen (TON) content of sediment as well as $\delta^{13}C$ of organic matter were measured on ground sample (~25 mg) with a FISONS NA 1500 NC elemental analyzer coupled with an Optima IR-MS. For $\delta^{13}C$, routine measurements are precise within 0.3‰. Isotopic measurements are expressed relative to VPDB standard using sucrose ($\delta^{13}C = -10.3 \pm 0.2‰$) as an internal standard.

Results

The principal results of the multi-proxy analysis are presented in Figure 4. Other results are discussed in the next chapter and presented in Figure 5.

Magnetic susceptibility values vary between 50×10^{-6} S.I. (8 cm) and 799×10^{-6} S.I. (13.5 cm), with an average of $124 \pm 100 \times 10^{-6}$ S.I. (Fig. 4a). The curve shows a decreasing trend from the base of the core to 15 cm. The highest values occur between 13 and 14 cm, in relation to a tephra layer (Fig. 5). Above 13 cm, values are low, with minima between 6 and 8 cm. Gamma density ranges between 1.18 and 1.49 g/cm^3 (average: 1.35 ± 0.08).

Bulk wet density varies between 0.64 and 1.36 g/cm^3 (average: 0.99 ± 0.16) and dry density ranges from 0.16 to 0.61 g/cm (average: 0.33 ± 0.09). The water content of the samples (LOI_{105}) varies between 38.6% and 75.5%

(average: 67.1 ± 6.0%) with the lower value (38.6%) occurring at 13.5 cm. Results from loss on ignition at 550°C range from 1.83% to 10.29% (average: 8.19 ± 1.41%) with the lowest value (1.83%) occurring at 13.5 cm depth.

The mean grain size (Fig. 4b) ranges between 13 µm (5 cm) and 49 µm (13.5 cm). The average is 20.7 ± 5.0 µm. Values are low and constant below 22 cm, except for the coarse tephra layer at 43.25 cm. They increase between 22 and 6 cm, with a maximum at 13.5 cm, related to a tephra layer. Values are low for the two green clayey layers. From 6 to 0 cm, the grain size curve shows a coarsening upward.

Bulk mineralogy consists of amorphous particles (volcanic glass, amorphous clay minerals, biogenic silica and organic matter), plagioclase and pyroxene (Fig. 4c). Quartz and olivine are secondary minerals. Mineralogy does no vary significantly with depth, except for the tephra layer at 13.5 cm that is rich in crystallized minerals.

Bulk geochemistry data show Al_2O_3 values ranging from 9.3% to 16.4% (average: 12.8 ± 1.5%), TiO_2 ranging from 0.62% to 0.94% (average: 0.78 ± 0.08%) and biogenic silica determined by normative calculation from 4.0% to 42.8% (average: 23.9 ± 7.3%) (Figs. 4d and e) if we admit a SiO_2/Al_2O_3 ratio of 3.5 for the terrigenous sediments (see next chapter). Curves show a decreasing trend of terrigenous elements and an increasing trend of biogenic silica between the base of the core and 14 cm. Between 13 and 14 cm, biogenic silica content is close to 0 and terrigenous elements concentrations are maxima. This is followed by a decrease of terrigenous elements content and an increase of biogenic silica content between 13 and 6 cm. Finally, between 6 and 0 cm, biogenic silica values decrease, with a minimum at 2-3 cm whereas terrigenous elements curves show the opposite trend.

The biogenic silica content determined by wet alkaline extraction varies between 13.0% and 35.3% (average: 24.1 ± 5.5%).

TOC and TON curves are parallel and values generally decrease with depth (Fig. 4f). Values for TOC range from 0.6% to 3.6% (average: 2.50 ± 0.59%) and TON ranges from 0.05% to 0.33% (average: 0.23 ± 0.05%). Minimum values occur at 13-14 cm. The C/N atomic ratio does not vary significantly, ranging from 11.2 to 14.7 (average: 12.8 ± 0.8%). Finally, $\delta^{13}C$ values range from -27.3‰ to -29.0‰ with higher values between 46 and 29 cm (Fig. 4g). $\delta^{13}C$ results decrease from 29 cm to a minimum value at 14 cm. In the upper part of the core, values increase.

Figure 4: Multi-proxy results obtained on PU-II-P5 short core, (a) Magnetic susceptibility; (b) grain size (both are depth adjusted from PU-II-P1); (c) bulk mineralogy; (d) Al_2O_3 and TiO_2 concentrations; (e) biogenic silica concentration obtained by normative calculation based on XRF bulk geochemical data; (f) total organic carbon and total organic nitrogen content of the sediment; and (g) geochemical characteristics of the organic matter ($\delta^{13}C$ and C/N atomic ratio). Mineral proportions were estimated by measuring the intensity of the principal diffraction peak multiplied by a corrective factor from Cook et al. (1975): amorphous 3.7 Å, 75x; plagioclases 3.18-3.20 Å, 2.8x; pyroxenes 2.99-3.00 Å, 5x; olivine 2.45 Å, 5x; quartz 3.34 Å, lx.
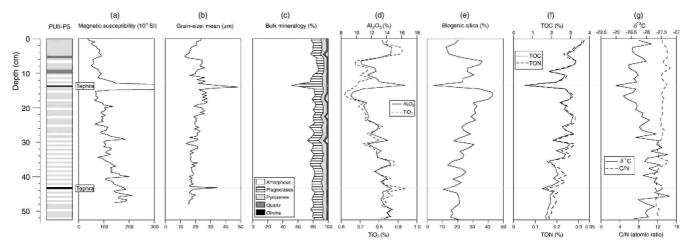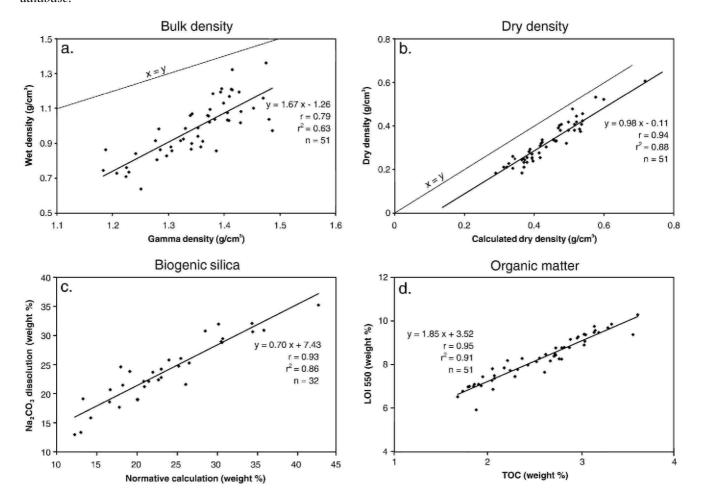
Figure 5: *Comparison of results obtained by 2 different methods for the estimation of the density, biogenic silica and organic matter concentrations, (a) Density: humid weighted density vs. gamma bulk density; (b) dry density: weighted vs. calculated from gamma density; (c) biogenic silica: Na_2CO_3 dissolution vs. XRF normative calculation; and (d) organic matter content: TOC vs. LOI_{550}. Samples containing tephras were removed from the database.*

Comparison between measurement methods for density, organic matter and biogenic silica contents

For the measurement of sediment density and concentrations in organic matter and biogenic silica, we applied two different methods. This chapter compares the data obtained from these measurements in order to select the most appropriate method for both short (this paper) and long (Bertrand, 2005) sedimentary records.

Density

In order to calculate mass accumulation rates (MARs), dry density values were deduced from gamma density measurements. Gamma density theoretically corresponds to bulk wet density of the sediment (Breitzke, 2000). For PU-II short core samples, the gamma density (GD) and the measured wet density data are well correlated ($r^2 = 0.63$, $P < 0.0001$) but measured wet densities are systematically lower than gamma density values (Fig. 5a). We use the water content of samples to calculate the dry density from gamma density data (DDγ) as follows:

$$DD\gamma = GD \times (100 - LOI_{105}) \times 10^{-2}$$

The calculated dry densities are highly correlated with measured dry densities ($r^2 = 0.88$, $P < 0.0001$) but are systematically higher by 0.11 units (Fig. 5b). After subtraction of 0.11 units, dry density values calculated from gamma density measurements on Lago Puyehue sediments can thus be used as dry density for MAR calculation.

Biogenic silica concentration

Biogenic silica content of the sediment can be measured in three different ways: alkaline extraction (DeMaster, 1981; Mortlock and Froelich, 1989), normative calculation from bulk geochemical data (Leinen, 1977) or X-ray diffraction (Eisma and van der Gaast, 1971). Because the amorphous diffraction band on X-ray spectra of our samples, usually quantified for biogenic silica content, is also influenced by volcanic glasses, amorphous clays and organic matter, X-ray diffraction method cannot be used for biogenic silica quantification. We applied alkaline extraction and normative calculation methods to 32 samples. Biogenic silica concentrations derived from the alkaline extraction method ranges between 13.0% and 35.3%. Normative calculation results depend on the SiO_2/Al_2O_3 ratio of the lacustrine terrigenous particles, expected to originate from regional volcanic soils and rocks. Our results on watershed soil sediments show a SiO_2/Al_2O_3 ratio of 2.47 ± 0.60 (range 1.77-3.41; Bertrand, 2005) and results obtained on volcanic rocks are 4.73 ± 0.41 (range 3.74-5.15; Gerlach et al., 1988). We chose a mean value of 3.5 as representative of the SiO_2/Al_2O_3 ratio of terrigenous sediments. This value is close to the reference values generally admitted for continental crust, i.e., 3.4 with extremes of 2.8 and 3.9 (Leinen, 1977; Robinson, 1994; Peinerud, 2000). This choice is supported by the strong correlation ($r = 0.86$, $P < 0.0001$) between normative calculation and alkaline extraction methods (Fig. 5c). The linear regression between both methods (Fig. 5c) has a *y*-intercept of 7.4. This value represents the silica dissolved by Na_2CO_3 but not calculated as biogenic silica by normative calculation. This is due to dissolution of volcanic glass and/or amorphous clays during the alkaline extraction of biogenic silica. Indeed, alkaline extraction on soil samples provide 4-11.5% of dissolved silica (mean: 7.9%). Normative calculation method based on XRF bulk geochemical results is selected for its rapidity.

Organic matter content

The concentration of total organic carbon (TOC) is a fundamental parameter to describe the organic matter content of the sediment. It represents the fraction of organic matter that escaped remineralization during sedimentation. However, loss on ignition at 550°C during 4 h (LOI_{550}) is also used to estimate sediment organic matter content (Herri et al., 2001). Correlation between both methods is usually good ($r > 0.95$; Dean, 1974; Brauer et al., 2000; Santisteban et al., 2004). Typical organic matter contains roughly 50% of carbon, so LOI values are about twice the TOC values. Our results give a high correlation coefficient ($r = 0.95$, $r^2 = 0.91$, $P < 0.0001$) if we admit a linear correlation (Fig. 5d), with a 1.85 slope, signifying that organic matter of PU-II sediments contains 54% of carbon. We also note that our results of TOC/LOI perfectly agree with Boyle's data (2001), suggesting lower errors in estimation of organic content by LOI_{550} for organic-rich sediments.

Discussion

Relationship between paleoenvironmental proxies and sedimentological data

The sedimentological and geochemical analyses carried on PU-II short core provide a continuous record of limnological changes in Lago Puyehue for the last 600 yr.

Several proxies depict parallel trends (Fig. 4): (1) Absolute magnetic susceptibility (MS) values are high because the sediment is composed of volcanic particles rich in magnetic minerals. These values are positively correlated with Al_2O_3 and TiO_2 concentrations (Table 2). Moreover, MS data are negatively correlated with the biogenic silica and organic matter contents (Table 2). This suggests that magnetic susceptibility can be used as a proxy for the terrigenous/biogenic particles ratio. (2) Except for the tephra layers, the grain size data are positively correlated with the biogenic silica content ($r = 0.63$) because the coarse sediment fraction consists of diatoms while the fine sediment fraction consists of detrital particles. Grain size is thus a proxy for the biogenic content of the sediment. It is negatively correlated with magnetic susceptibility and terrigenous elements (Table 2).

Table 2: *Correlation coefficients (r) between different proxies measured on PU-II short core*

	MS	GS	Al_2O_3	TiO_2	SiO_2 bio	LOI_{550}
MS	1.00					
GS	-0.36	1.00				
Al_2O_3	0.42	-0.64	1.00			
TiO_2	0.40	-0.67	0.94	1.00		
SiO_2 bio	-0.41	0.63	-0.99	-0.95	1.00	
LOI_{550}	-0.69	0.18	-0.42	-0.32	0.41	1.00

MS	**GS**	**Al$_2$O$_3$**	**TiO$_2$**	**SiO$_2$ bio**	**LOI$_{550}$**

MS: magnetic susceptibility; GS: grain size; Al$_2$O$_3$ and SiO$_2$: concentrations of these elements in the sediment; SiO$_2$ bio: biogenic silica concentration; LOI$_{550}$: loss on ignition at 550°C. Samples containing tephras were removed from the database.

The only proxy measured on all the short cores collected in Lago Puyehue is the magnetic susceptibility (Fig. 2). Figure 2 demonstrates that the four short cores collected outside the influence of underflow currents present the same magnetic susceptibility trends. Values show a decreasing trend from the bottom of the core until the A.D. 1921-1922 tephra layer (i.e., increasing biogenic/ terrigenous ratio). Then, values are lower between A.D. 1921-1922 and A.D. 1960 and finally increase from A.D. 1960 to present-day. This argues that changes in the terrigenous/biogenic ratio described in the PU-II core are valid for the whole lake.

The main event identifiable by each proxy is the tephra layer related to the 1921-1922 eruption of Puyehue-Cordon de Caulle at 13.5-13.8 cm (Fig. 4). The sample containing this layer presents high values of magnetic susceptibility and grain size, high concentration of crystallized minerals and terrigenous elements and low contents of biogenic silica and organic matter. The tephra layer at 43-43.5 cm is only observed by its coarse grain size and low content of organic matter and biogenic silica. The MS value associated with this tephra layer is close to MS values of the host sediment.

Green clay layers probably originate from the *in situ* alteration of pumice, as suggested by their high glass content and frequent pumice fragments identified in these deposits. Occurrence of such layers represents remains of volcanic sediments. Lacustrine sediment overlaying green clayey layers is always finer than usual, especially for the layer at 5-5.5 cm. This is due to a decrease of the total diatom content of the sediment, mainly caused by a decrease in *Cyclotella* (M. Sterken, unpublished data).

The bulk mineralogy (Fig. 4c) is similar to the mineralogy of regional volcanic ash soils (Bertrand, 2005), however, enriched in amorphous particles because of the high diatom content of the sediment. This confirms that the detrital sediment originates from the local volcanic watershed.

Interpretation of geochemical results

The biogenic silica content of sediment represents the siliceous skeletal matter from the epilimion, minus the dissolution that occurs during settling and on the lake floor (Cohen, 2003). Assuming that dissolution is proportional to primary biogenic production, biogenic silica can be interpreted in terms of overall paleoproductivity. This is particularly true for lakes in volcanic environment (Si-rich) where diatoms are the main autochthonous biogenic product. Results on the PU-II long core show that volcanic eruptions do not influence the biogenic productivity of the lake (M. Sterken, unpublished data). Biogenic paleoproductivity is thus directly related to climate changes. Absolute biogenic silica values are high (max: 42.8%) and we do not observe any dissolution evidence.

On the contrary, the general decreasing trend of organic matter content with depth can be partially due to organic matter remineralization. The upper values follow a classical exponential diagenetic profile (Zimmerman and Canuel, 2002). The close to constant C/N ratios enable us to deduce that proportions of algal and land-plant organic matter remains constant with time. The C/N atomic ratio is low and suggests that organic matter contained in sediments is mainly produced in the lacustrine environment. This is consistent with the relatively large lake size (164 km^2).

The carbon isotopic composition of organic matter in lake sediments is mainly influenced by organic matter sources and paleoproductivity rates (Meyers and Teranes, 2001). Because C/N ratios are constant throughout the core, we reject variations in organic matter sources to be the cause of isotopic variability. Observed δ^{13}C variations are thus related to changes of paleoproductivity. Because phytoplankton (C3 algae) preferentially uses C to produce organic matter, sedimentation of algal organic matter consequently removes ^{12}C from surface-water (Meyers, 2003). Increased productivity therefore yields an increase in the δ^{13}C of organic matter produced in lakes (Meyers, 2003). This increase in productivity could be related either to climate improvement or to higher nutrient availability, mainly nitrates and phosphates derived from soil erosion (Meyers and Teranes, 2001).

Mass accumulation rates calculation

In order to avoid interpretation errors due to dilution of elements by other sedimentary components, we calculated mass accumulation rates (MARs) as follows:

$$MAR_{elt} = SR \times DD \times [elt] \times 10^2$$

with MAR_{elt}: mass accumulation rate of the considered element in g m^{-2} yr^{-1}; SR: sedimentation rate in cm yr^{-1}; DD: dry density in g/cm^3; and [elt] : the concentration of the considered element in %. We consider sediment made of three components: terrigenous particles, organic matter and biogenic silica. Therefore, we calculated MARs for each component:

$$MAR_{SiO_2\ bio} = SiO_2\ bio \times SR \times DD \times 10^2$$

$$MAR_{OM} = LOI_{550} \times SR \times DD \times 10^2$$

$$MAR_{ter} = (100 - SiO_2\ bio - LOI_{550}) \times SR \times DD \times 10^2$$

with $MAR_{SiO2\ bio}$; MAR_{OM} and MAR_{ter}: the mass accumulation rates of biogenic silica, organic matter and terrigenous particles, respectively, in g m^{-2} yr^{-1}; SiO_2 bio: the concentration in biogenic silica in %; and LOI_{550}: the loss on ignition at 550°C in %.
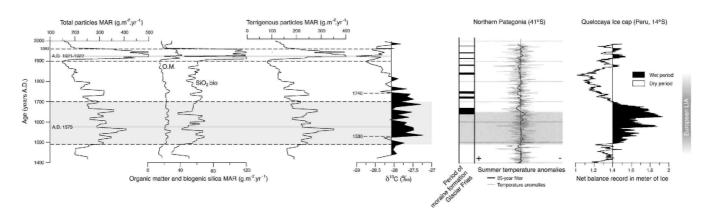
Total MAR shows high values between A.D. 1490 and A.D. 1700 as well as between A.D. 1920 and A.D. 1960 (Fig. 6). Throughout the core, the biogenic silica and organic matter MAR do not vary significantly, except before A.D. 1490 and for the A.D. 1920-1960 interval. Five periods can be identified, mainly based on variations of the terrigenous MAR:

(1) Before A.D. 1490: the biogenic silica and terrigenous particles MARs are low.
(2) A.D. 1490-1700: terrigenous particles MAR are higher than average.
(3) A.D. 1700-1900: decrease of terrigenous particles MAR.
(4) A.D. 1900-1960: high MARs for the three sediment components.
(5) After A.D. 1960: the MARs show values similar to the A.D. 1850-1900 period, with exceptionally low biogenic silica MAR.

High biogenic silica and organic matter MARs are interpreted as a high lake paleoproductivity. High terrigenous MAR results from high erosion of lake watershed, linked either to important precipitations or higher sediment availability in the lake catchment.

For the A.D. 1490-1700 period, high terrigenous MARs are interpreted to be caused by a wet climate, resulting in higher catchment erosion and an increasing lake terrigenous supply. High δ^{13}C values and organic matter MAR attest for a higher productivity during A.D. 1530-1740 (Fig. 6). This probably results from the high nutrient supply during A.D. 1490-1700, with a temporal shift of ~ 40 yr. δ^{13} C data lag nutrients delivery by ~ 40 yr because the uptake of ^{12}C from lake waters lasts several decades before being sufficiently large to be registered in lake sediments.

Figure 6: Mass accumulation rates and δ^{13}C data of PU-II-P5 short core, compared with data from the Southern Hemisphere. Quelccaya Ice Cap from Thompson et al., 1985. Northern Patagonia from Luckman and Villalba, 2001. Black lines correspond to periods of moraine formation.

The A.D. 1700-1900 period is characterized by a decrease of terrigenous particles MAR. The minimum of terrigenous particles MAR corresponds to a minimum of δ^{13}C at A.D. 1890-1900. For the last 600 yr, the A.D.

1800-1900 period seems to be the period with the lowest precipitation, and lower paleoproductivity due to low nutrient supply, with a minimum at A.D. 1890-1900 (Fig. 6). These characteristics agree with a drying climate for the A.D. 1700-1900 period.

The interpretation of the high MARs during the A.D. 1900-1960 period, in particular between A.D. 1920 and A.D. 1960, is doubtful. Two volcanic/seismic events encompass this period: the 1921-22 eruption of Puyehue-Cordon de Caulle and the 1960 earthquake of Valdivia. Moreover, this period corresponds to the onset of the lake level regulation. High MARs during this interval most probably result from the high sediment availability in the watershed due to the intensified volcano/seismic activity, but can also be modified by an anthropogenic influence.

After 1960 A.D., organic matter and terrigenous MAR return back to average values suggesting the end of the tectonic and seismic instabilities. The low biogenic silica MAR relates the absence of lake eutrophication. This is confirmed by the constant C/N ratio for the whole core attesting for the absence of land reclamation.

Comparison with Southern Hemisphere records

Our data demonstrate the occurrence of a wet period during A.D. 1490-1700 followed by a drying climate during A.D. 1700-1900. These results fit with several evidences from the literature (Fig. 6).

In Northern Patagonia (41°S, Chile and Argentina), Villalba (1990) recognized two periods of general glacial advances: A.D. 1270-1380 and A.D. 1520-1670. By a tree-ring study in the same area, Lara and Villalba (1993) and Villalba (1994) evidenced a long interval with below-average temperatures from A.D. 1490 to A.D. 1700 and the most recent warm periods from A.D. 1720 to A.D. 1750 and A.D. 1800 to A.D. 1880. The coincidence of periods with low temperatures and glacial advances is manifest. Glacial advances during the last millennium seem to be related to a combination of higher precipitation and lower temperatures (Villalba, 1994). More recently, a tree-ring study by Villalba et al. (2001) of 17 records from Northern Patagonia demonstrates a long cold interval extending from ca. A.D. 1500 to A.D. 1660 (Fig. 6).

Jenny et al. (2002) described high flood periods at 34°S during the A.D. 1300-1700 and A.D. 1850-1998 intervals. These periods are linked to moisture increase due to strengthening of the Westerlies.

In Peru, Quelccaya ice cap data (14°S) present high snow accumulation rates during the A.D. 1500-1720 period (Thompson et al., 1985, 1986; Fig. 6). This interval is interpreted as the wettest period of the last millennium, at the onset of the LIA. It is followed by a dry period at A.D. 1720-1860. Moraines deposited before A.D. 1650 were described close the Quelccaya ice cap (Goodman et al., 2001).

The wet interval deduced from Lago Puyehue sediments during the A.D. 1490-1700 period is strikingly consistent with higher ice accumulation rates in the Quelccaya ice core (Thompson et al., 1985), as well as with colder temperatures deduced from tree-ring evidence in Northern Patagonia (Luckman and Villalba, 2001). The drying climate deduced from our results from ~A.D. 1740 to A.D. 1900 corresponds with the most recent dry periods of Lara and Villalba (1993).

These results emphasize that precipitation changes during the last 600 yr in Southern America seem to be contemporaneous. All these observations demonstrate a strengthening of the Westerlies north of 50°S during the A.D. 1490-1700 period. This would have increased the moisture and precipitation in the Andes leading to an increased terrigenous particles supply in regional lakes.

In the Northern Hemisphere, the Little Ice Age (LIA) was characterized by colder temperatures and glacial advances. Its onset is dated between A.D. 1430 and A.D. 1550 and its end between A.D. 1700 and A.D. 1850, with a general agreement for the A.D. 1550-1850 interval (Bradley et al., 2003). The recent literature review of Soon and Baliunas (2003) attests for an interhemispheric presence of the LIA. Our results do not show significant paleoproductivity changes in favor of a cooler climate. However, the high rainfall reconstructed for the A.D. 1490-1700 period could be the local signature of the onset of the LIA. At the same latitude, Lamy et al. (2001) described increased rainfall interpreted as an equatorward shift of the Southern Westerlies paralleling the LIA. These results evidence that the Southern Hemisphere LIA could have been initiated by a wet climate contemporaneous with the beginning of the Northern Hemisphere cold period. Other records from South America (< 40°S) have demonstrated that this high precipitation period was accompanied by cold temperatures until the end of the 19th century (Thompson et al., 1985, 1986; Luckman and Villalba, 2001, Valero-Garcés et al., 2003). Further South, in Gran Campo Nevado (53°S), major glacial advances are dated from the 1870s,

reflecting probably the end of the Southern Hemisphere LIA (Koch and Kilian, 2005). The end of the cold period is ambiguous and seems to vary with latitude. In Tierra del Fuego (55°S), the LIA seems to be absent (Mauquoy et al., 2004).

Conclusion

Lacustrine sediments of Lago Puyehue contain a high-resolution record of precipitation changes in Southern Chile. We demonstrate that dry-density data can be inferred from gamma density measurements after correction of the sediment water content. Moreover, we show that LOI_{550} and normative calculation based on bulk XRF geochemical results are reliable estimates of organic matter and biogenic silica concentrations, respectively. For the last 600 yr, precipitation rather than temperature seem to influence the Lago Puyehue sedimentation and, in particular, the terrigenous particles mass accumulation rate. Our results agree with a humid climate between A.D. 1490 and A.D. 1700, resulting in high watershed erosion and subsequent high terrigenous particles supply. At the same time, lake paleoproductivity slightly increased due to the high nutrients supply. This humid period seems to be the local signature of the onset of the LIA. Contemporaneous humidity changes, marking the initiation of the Little Ice Age, have been documented in the Quelccaya ice cap record in Peru. During the A.D. 1740-1900 interval, humidity decreased but the climate remained cold. Our results support the fact that the Little Ice Age was a global event, not only restricted to the Northern Hemisphere.

Acknowledgments

References

Bentley, M.J., 1997. Relative and radiocarbon chronology of two former glaciers in the Chilean Lake District. Journal of Quaternary Science 12, 25-33.

Bertrand, S., 2005. Sédimentation lacustre postérieure au Dernier Maximum Glaciaire dans les lacs Icalma et Puyehue (Chili méridional): Reconstitution de la variabilité climatique et des évènements sismo-tectoniques. PhD dissertation, University of Liège, Belgium, 154 p.

Bologne, G., Duchesne, J.C., 1991. Analyse des roches silicatées par spectrométrie de fluorescence X: précision et exactitude. Professional Paper, Belgian Geological Survey 249, 11 pp.

Boyle, J.F., 2001. Inorganic geochemical methods on palaeolimnology. In: Smol, J.P. (Ed.), Tracking Environmental Change Using Lake Sediments. Kluwer Academic Publishers, Dordrecht, pp. 83-141.

Bradley, R.S., Briffa, K.R., Cole, J., Hugues, M.K., Osborn, T.J., 2003. The climate of the Last Millenium. In: Pedersen, T.S. (Ed.), Paleoclimate, Global Change and the Future. Springer, Berlin, pp. 105-141.

Brauer, A., Mingram, J., Frank, U, Günter, C, Schettler, G, Wulf, S., Zolitscka, B., Negendank, J.F., 2000. Abrupt environmental oscillations during the early Weichselian recorded at Lago Grande di Monticchio, Southern Italy. Quaternary International 73/74, 79-90.

Breitzke, M., 2000. Physical properties of marine sediments. In: Zabel, M. (Ed.), Marine Geochemistry. Springer, Berlin, pp. 29-72.

Brindley, G.W., Brown, G, 1980. Crystal Structures of Clay Minerals and Their X-ray Identification, Monograph-Mineralogical Society (London), vol. 5, 495 pp.

Campos, H., Steffen, W., Agüero, G, Parra, O., Zúñiga, L., 1989. Estudios limnologicos en el Lago Puyehue (Chile): morfometria, factores fisicos y quimicos, plancton y productividad primaria. Medio Ambiente 10, 36-53.

Cohen, A.S., 2003. Paleolimnology: The History and Evolution of Lake Systems. Oxford Univ. Press, New York. (528 pp).

Committee on Abrupt Climate Change, 2002. Abrupt Climate Change: Inevitable Surprises. National Academy Press, Washington, DC (244 pp).

Cook, H.E., Johnson, P.D., Matti, J.C., Zemmels, I., 1975. Methods of sample preparation and X-ray diffraction data analysis, X-ray mineralogy laboratory. In: Kaneps, A.G (Ed.), Initial Reports of the DSDP, Washington DC, pp. 997-1007.

Dean, W.E., 1974. Determination of carbonate and organic matter in calcareous sediments and sedimentary rocks by loss on ignition: comparison with other methods. Journal of Sedimentary Petrology 44, 242-248.

DeMaster, D.J., 1981. The supply and accumulation of silica in the marine environment. Geochimica et Cosmochimica acta 45, 1715-1732.

Eisma, D., van der Gaast, S.J., 1971. Determination of opal in marine sediments by X-ray diffraction. Netherlands Journal of Sea Research 5, 215-225.

Folk, R.L., Ward, W.C., 1957. Brazos river bar: a study in the significance of grain size parameters. Journal of Sedimentary Petrology 27, 3-26.

Gerlach, D.C., Frey, F.A., Moreno-Roa, H., Lopez-Escobar, L., 1988. Recent volcanism in the Puyehue-Cordon Caulle Region, Southern Andes, Chile (40.5°S): petrogenesis of evolved lavas. Journal of Petrology 29, 333-382.

Goodman, A.Y., Rodbell, D.T., Seltzer, G.O., Mark, B.G, 2001. Subdivision of glacial deposits in Southeastern Peru based on pedogenic development and radiometric ages. Quaternary Research 56,31-50.

Heiri, O., Lotter, A.F., Lemcke, G, 2001. Loss on ignition as a method for estimating organic and carbonate content in sediments: reproductibility and comparability of results. Journal of Paleolimnology 25, 101-110.

Heusser, C.J., 2003. Ice Age Southern Andes—A Chronicle of Palaeoecological Events. Elsevier, Amsterdam (230 pp).

Jenny, B., Valero-Garcés, B.L., Urrutia, R., Kelts, K., Veit, H., Appleby, P.G, Geyh, M., 2002. Moisture changes and fluctuations of the westerlies in Mediterranean Central Chile during the last 2000 years: the Laguna Aculeo record (33°50'S). Quaternary International 87, 3-18.

Koch, J., Kilian, R., 2005. 'Little Ice Age' glacier fluctuations, Gran Campo Nevado, southernmost Chile. The Holocene 15 (1), 20-28.

Lamy, F., Hebblen, D., Röhl, U, Wefer, G, 2001. Holocene rainfall variability in Southern Chile: a marine record of latitudinal shifts of the Southern Westerlies. Earth and Planetary Science Letters 185, 369-382.

Lara, A., Villalba, R., 1993. A 3620-year temperature record from *Fitzroya cupressoides* tree rings in Southern South America. Science 260, 1104-1106.

Laugenie, C, 1982. La région des lacs, Chili méridional. PhD dissertation, Université de Bordeaux III. 822 pp.

Leinen, M., 1977. A normative calculation technique for determining opal in deep-sea sediments. Geochemica et Cosmochimica Acta 41, 671-676.

Luckman, B.H., Villalba, R., 2001. Assessing the synchroneity of glacier fluctuations in the western cordillera of the Americas during the last illennium. In: Markgraf, V. (Ed.), Interhemispheric Climate Linkages, an Diego, pp. 119-140.

Markgraf, V, 2001. Interhemispheric Climate Linkages. Academic Press, an Diego (454 pp).

Mauquoy, D., Blaauw, M., van Geel, B., Borromei, A., Quattrocchio, M., hambers, F.M., Possnert, G, 2004. Late Holocene climatic changes in Tierra del Fuego based on multiproxy analyses of peat deposits. Quaternary Research 61, 148-158.

Meyers, P.A., 2003. Applications of organic geochemistry to paleolimnological reconstructions: a summary of examples from the Laurentian Great Lakes. Organic Geochemistry 34, 261-289.

Meyers, P.A., Teranes, J.L., 2001. Sediment organic matter. In: Last, M., Smol, J. (Eds.), Tracking Environmental Change Using Lake Sediments. Kluwer Academic Publishers, Dordrecht, pp. 239-269.

Miller, A., 1976. The climate of Chile. In: Schwerdtfeger, W. (Ed.), World Survey of Climatology. Elsevier, Amsterdam, pp. 107-134.

Mortlock, R.A., Froelich, P.N., 1989. A simple method for the rapid determination of biogenic opal in pelagic marine sediments. Deep-sea Research 36, 1415-1426.

Muñoz, M., 1980. Flora del parque nacional Puyehue, Universitaria, Santiago (557 pp). Parada, M.G, 1973. Pluviometria de Chile. Isoyetas de Valdivia-Puerto Montt. CORFO, Departamento de Recursos Hydraúlicos. Santiago, Chile, 73 pp.

Peinerud, E.K, 2000. Interpretation of Si concentrations in lake sediments: three case studies. Environmental Geology 40, 64-72.

Robinson, C, 1994. Lago Grande di Monticchio, southern Italy: a long record of environmental change illustrated by sediment geochemistry. Chemical Geology 118, 235-254.

Santisteban, J.I., Mediavilla, R., López-Pamo, E., Dabrio, C.J., Zapata, B.L., Garcia, J.G., Castaño, S., Martiínez-Alfaro, P.E., 2004. Loss on ignition: a qualitative or quantitative method for organic matter and carbonate mineral content in sediments? Journal of Paleolimnology 32 (3), 287-299.

Soon, W., Baliunas, S., 2003. Proxy climatic and environmental changes of the past 1000 years. Climate Research 23, 89-110.

Thompson, L.G., Mosley-Thompson, E., Bolzan, J.F., Koci, B.R., 1985. A 1500-year record of tropical precipitation in ice cores from the Quelccaya ice cap, Peru. Science 229, 971-973.

Thompson, L.G, Mosley-Thompson, E., Dansgaard, W., Grootes, P.M., 1986. The Little Ice Age as recorded in the stratigraphy of the tropical Quelccaya ice cap. Science 234, 361-364.

Valero-Garcés, B.L., Delgado-Huertas, A., Navas, A., Edwards, L., Schwalb, A., Ratto, N., 2003. Patterns of regional hydrological variability in central-southern Altiplano (18°S-26°S) lakes during the last 500 years. Palaeogeography, Palaeoclimatology, Palaeoecology 194, 319-338.

Villalba, R., 1990. Climatic fluctuations in Northern Patagonia during the last 1000 years as inferred from tree-ring records. Quaternary Research 34, 346-360.

Villalba, R., 1994. Tree-ring and glacial evidence for the medieval warm epoch and the little ice age in Southern South America. Climatic Change 26, 183-197.

Villalba, R., D'Arrigo, R.D., Cook, E.R., Jacoby, G.C., Wiles, G, 2001. Decadal-scale climatic variability along the extratropical western coast of the Americas: evidence from tree-ring records. In: Markgraf, V (Ed.), Interhemispheric Climate Linkages. Academic Press, San Diego, pp. 155-172.

Zimmerman, A.R., Canuel, A., 2002. Sediment geochemical records of eutrophication in the mesohaline Chesapeake Bay. Limnology and Oceanography 47 (4), 1084-1093.